Proceedings of the
Annual Stability Conference
Structural Stability Research Council
Nashville, Tennessee, March 24-27, 2015

Composite Action in Global Buckling of Built-Up Columns Using Semi-Analytical Fastener Elements

David C. Fratamico[1], Shahabeddin Torabian[2], Benjamin W. Schafer[3]

Abstract

In this paper, a semi-analytical model for steel-to-steel screw fasteners is derived and implemented to calculate the elastic global flexural buckling of built-up members. In cold-formed steel design, the modified slenderness ratio approach of AISI-S100-12 Section D1.2 does not explicitly account for fastener stiffness and layout in built-up members. This work explores a new design philosophy in which the stiffness of fasteners is directly included in the determination of the elastic buckling determination and that same stiffness is used to explore the distribution of force amongst the fasteners in a built-up member undergoing deformations consistent with flexural buckling. A "2D fastener element" is derived and provides a means to use direct axial, shear, and bending stiffness of a fastener in an element stiffness compatible with beam element models of the members, which comprise a built-up section. Verification for the element was supported through analyses in ABAQUS and in MASTAN2 using the same fundamental mechanism on which the new, efficient fastener element stiffness matrix is based. A parametric study was performed where fastener stiffness and spacing were varied for a built-up member type. The study confirms that the fastener element yields stable elastic buckling solutions and reveals the sensitivity of global flexural buckling to the shear stiffness of the screw fasteners that create typical built-up cold-formed steel members. The level of partially composite action in global flexural buckling is obtained numerically, including the effect of fastener layout and stiffness, and this framework is proposed for flexural elastic buckling determination of cold-formed steel built-up columns. Potentials for modeling nonlinear fastener behavior, prospects for built-up member testing, and extensions to Finite Strip modeling of cold-formed steel built-up members are also discussed as future research to support the overall goal of developing advanced methods for designing cold-formed steel built-up members.

1. Introduction

Cold-formed steel (CFS) structural systems are composed of thin-walled open sections that have high capacity while also being lightweight. In many parts of low to mid-rise CFS structures, higher axial capacity or local frame rigidity is often required, necessitating the use of built-up sections. Common built-up members include the screw-fastened back-to-back "I" and toe-to-toe

[1] Graduate Research Assistant, Dept. of Civil Engineering, Johns Hopkins University, <fratamico@jhu.edu>
[2] Assistant Research Scientist, Dept. of Civil Engineering, Johns Hopkins University, <torabian@jhu.edu>
School of Civil Engineering, College of Engineering, University of Tehran, <torabian@ut.ac.ir>
[3] Professor and Chair, Dept. of Civil Engineering, Johns Hopkins University, <schafer@jhu.edu>

"box" sections, which are doubly symmetric, constructed using industry standard steel-to-steel screws and lipped channel sections, and offer an axial compression capacity more than twice that of the individual members. Their current use includes, but is not limited to, shear wall chord studs, end studs on orthogonally intersecting walls, headers, and jambs.

Historically, built-up hot-rolled steel sections were popular in steel bridge trusses and high-rise structures. Whether of laced or battened type, these members' capacities and deformation behaviors were extensively studied by Engesser, Bleich, Timoshenko, and others. However, work in this basic area continues today. Analytical expressions have been developed based on Bleich's predictions, but for general boundary conditions and incorporating a separation ratio when calculating the overall section's moment of inertia (Aslani and Goel 1991). Others have looked at the compound buckling characteristics of laced and battened columns and developed formulae for critical buckling loads to account for shear deformation in the built-up flange components, geometric imperfections, and local-global buckling interactions (Duan et al. 2002). Liu et al. (2009) experimentally validated the AISC-360 (2010) provision that the slenderness ratio of an individual element in a built-up column should not exceed three-fourths the overall member slenderness ratio.

Design rules for built-up CFS members are limited in the current North American cold-formed steel specification (AISI-S100 2012), yet current research is working to expand understanding of their behavior. Experimental studies on back-to-back CFS channel sections found that the AISI-S100 (2012) modified slenderness ratio can be conservative for certain sections and that shear slip resistance at the end connections is critical for global column strength (Stone and LaBoube 2005). Young and Chen (2008) conducted experiments on built-up CFS sections with intermediate stiffeners and found that using the Direct Strength Method (DSM) for calculating the local and distortional elastic buckling strengths using only single section properties provided reliable and conservative estimates. Other experimental tests on conventional and innovative (roughly optimized) built-up CFS sections were completed and compression capacities were compared with DSM-based equations that were modified to accommodate global-distortional buckling interactions observed in tests (Georgieva et al. 2012). Loughlan and Yidris (2014) also investigated compound buckling in experiments for CFS sections while Kalochairetis and Gantes (2011) analytically and numerically studied the collapse behavior of laced steel columns with geometric imperfections, with both sets of authors studying global-local buckling interactions. Piyawat et al. (2011) explored nonlinear buckling of CFS built-up sections experimentally and compared with ANSYS and ABAQUS numerical results that overestimated inelastic buckling capacities observed in the tests. Li et al. (2014) completed a joint experimental and numerical analysis of 2 types of built-up CFS sections made with lipped and web-stiffened channel sections; one type had a back-to-back web configuration while the other contained overlapping flanges which were connected by screws. They proposed an axial strength prediction that extends existing AISI-S100 (2012) design provisions for global-flexural and distortional buckling, and offered practical guidelines on estimating optimal built-up member fastener spacing.

The 2005 AS/NZS standards require only a maximum fastener spacing requirement for CFS built-up column design (Zhang 2014). In the US, AISI-S100 (2012) Section D1.2 requires the calculation of the axial capacity of these columns using the modified slenderness ratio approach, as adopted from AISC 360 (2010).

$$\left(\frac{KL}{r}\right)_m = \sqrt{\left(\frac{KL}{r}\right)_o^2 + \left(\frac{a}{r_i}\right)^2} \quad (1)$$

where, $(KL/r)_o$ is the slenderness ratio of the whole composite section about its minor axis of buckling, a is the intermediate fastener spacing along the longitudinal length, and r_i is the minimum radius of gyration of the full, unreduced cross-sectional area of each single section within the built-up column. Eq. 1 is used to estimate the critical axial compressive load of built-up columns in minor-axis flexural buckling only. It does not, however, offer any insight on the effect of fastener spacing on torsional, flexural-torsional, distortional, or local buckling modes. In addition, the equation does not allow for consideration of the end conditions. Although, the code obliges the use of a special fastener grouping at the member ends, the requirement is prescriptive and its impact on the modified slenderness is not treated directly. Built-up members in general flexure are prescribed a maximum fastener spacing of the lesser of either $L/6$ or a factor dependent on the tensile strength of a single connection.

The work presented herein follows introductory work on the effects of fastener spacing on column buckling (Post 2014) and a previous, parametric numerical study in which the level of compositeness was varied using both fixed constraints and elastic springs as fasteners in Finite Element and Finite Strip-based models used for elastic buckling analyses (Fratamico and Schafer 2014). Although the partially composite realm was studied empirically in the past by Maia et al. (2012) and other researchers, this paper explores a design philosophy in which the level of compositeness (which is mostly influenced by the shear flexibility of connections, and fastener stiffness and spacing) is directly considered in the design of built-up CFS members. Considering the concept of general flexure (bending or global buckling of members) as a fundamental research focus, a two-dimensional finite element code was developed to model the partially composite behavior of built-up members, run parametric buckling and static analyses with varying fastener stiffness and spacing, numerically derive a generalized compositeness factor from a stability-based approach to design, estimate fastener shear flow along the length of built-up members, and introduce a single-element approximation for built-up members undergoing flexural buckling in a finite element modeling domain.

2. Modeling Composite Action

In design, the concepts of non-composite (no interconnection between structural elements) and fully composite (full interconnectivity between elements) are widely understood by engineers. For a built-up section, effective section properties are needed to determine the approximate flexural, torsional, or shear rigidity of the composite/built-up section. However, the concept of shear transfer between discretely connected components is often difficult to calculate, unless approximations based on empirical results are used. The following sections outline a new approach to quantifying partially composite behavior in built-up members, with an analysis specific to global flexural buckling of cold-formed steel columns.

2.1 Quantifying Partially Composite Behavior

Partially composite behavior stems from the deformations occurring in shear transfer (typically via fasteners) from one component to another in a composite/built-up section. Realistic estimates of fastener stiffness, layout, and behavior are therefore required. The current modified

slenderness ratio from AISI-S100-12 has been proven to provide an acceptable prediction of column buckling (see Fratamico and Schafer (2014) and others) provided that certain prescriptive measures are taken in design, such as the addition of end fastener groupings near the column supports, limitations to fastener spacing along the length, and minimums for fastener strength relative to the maximum axial strength of the built-up column. However, this estimation of column slenderness does not accommodate the strength of fasteners (or their stiffness), it does not directly consider the end fastener groupings (which exist not only for enabling composite action, but also for other framing connection purposes), it is inconveniently tied to the effective length factor for determining column slenderness, and it is not generalized for more than just back-to-back CFS channel sections, such as more than two sections connected together or ones in which local or distortional may govern the capacity. The following approach includes numerical modeling to estimate the effective flexural rigidity for composite sections in elastic global flexural buckling given empirical fastener stiffnesses and explicit modeling of end fastener groupings.

2.2 Semi-Analytical Fastener Element

To efficiently model a fastener numerically, the authors sought the direct use of springs in a finite element modeling domain. For the general problem, fastener springs were first considered for all 6 degrees of freedom in a Cartesian space: the $+z$ coordinate defined as left to right, the $+y$ coordinate defined as down to up, and the $+x$ coordinate defined as out of the page, as dictated by the right-hand rule. The y coordinate is parallel to a member's neutral axis, while the z coordinate is parallel to the line connecting a singly-symmetric channel section's shear center and centroid. The six conceptual springs are defined in Table 1. Each stiffness type can be associated with a mode of local deformation in a given steel member as defined by Peköz (1990) and others, but they are not discussed in-depth herein.

Table 1: Cartesian springs considered for the fastener element

Variable	Description	Units
k_x	transverse in-plane of web	force / length
k_y	longitudinal in-plane of web	force / length
k_z	perpendicular out-of-plane of web	force / length
$k_{\varphi x}$	longitudinal tilting	force x length
$k_{\varphi y}$	transverse tilting	force x length
$k_{\varphi z}$	drilling	force x length

The six springs of Table 1 were simplified to the in-plane axial, shear, and rotational degrees of freedom of interest for a two-dimensional analysis, namely k_z, k_y, and $k_{\varphi x}$ as shown in Fig. 1. The fastener element assumes an offset of length L with the springs located at the center of this offset (i.e., $L/2$) by rigid bars. As shown in Fig. 1, the axial (z) degree of freedom is uncoupled from shear and bending (y, ϕ_{x1}). From simple equilibrium the stiffness matrix, Fig. 2, is derived.

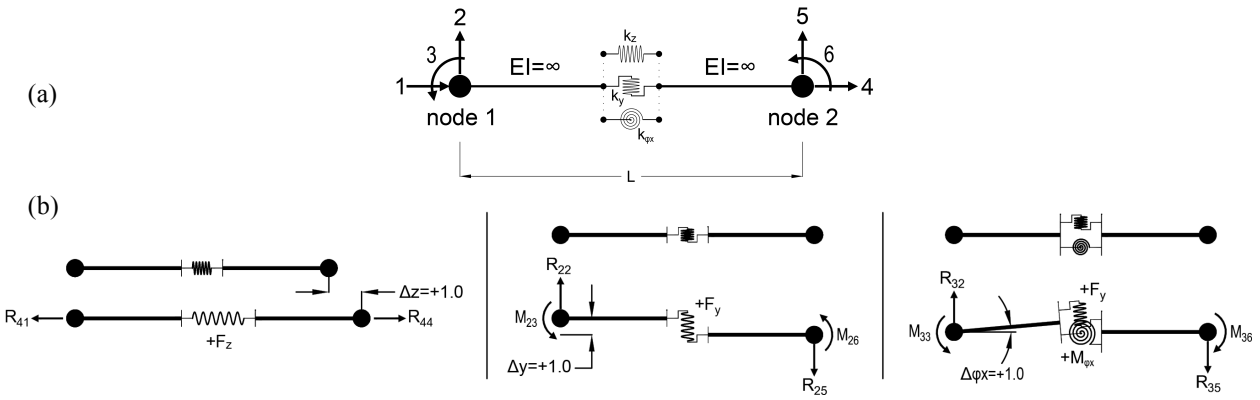

Figure 1: Two-dimensional fastener element showing (a) basic geometry and degrees of freedom and (b) axial, shear, and rotation free body diagrams

$$\begin{Bmatrix} F_{z1} \\ F_{y1} \\ M_{\phi x1} \\ F_{z2} \\ F_{y2} \\ M_{\phi x2} \end{Bmatrix} = \begin{bmatrix} k_z & 0 & 0 & -k_z & 0 & 0 \\ 0 & k_y & k_y\left(\frac{L}{2}\right) & 0 & -k_y & k_y\left(\frac{L}{2}\right) \\ 0 & k_y\left(\frac{L}{2}\right) & k_{\phi x} + k_y\left(\frac{L}{2}\right)^2 & 0 & -k_y\left(\frac{L}{2}\right) & -k_{\phi x} + k_y\left(\frac{L}{2}\right)^2 \\ -k_z & 0 & 0 & k_z & 0 & 0 \\ 0 & -k_y & -k_y\left(\frac{L}{2}\right) & 0 & k_y & -k_y\left(\frac{L}{2}\right) \\ 0 & k_y\left(\frac{L}{2}\right) & -k_{\phi x} + k_y\left(\frac{L}{2}\right)^2 & 0 & -k_y\left(\frac{L}{2}\right) & k_{\phi x} + k_y\left(\frac{L}{2}\right)^2 \end{bmatrix} \begin{Bmatrix} z_1 \\ y_1 \\ \varphi_{x1} \\ z_2 \\ y_2 \\ \varphi_{x2} \end{Bmatrix}$$

Figure 2: Direct stiffness equation for the fastener element

To verify the mechanics and results of this model, two steps were taken: basic check on the rigid mechanism in ABAQUS (2013) and comparison with a beam model in MASTAN2 (McGuire et al. 2000). ABAQUS (2013) was used to model the mechanism (i.e., 2 cantilevered rigid links connected with the 3 springs) using B31 beam elements with linear interpolation for the rigid links and global coordinate system-defined SPRING2 special purpose elements for the zero-length elastic springs. The same displacements were applied to the mechanism, and spring stiffnesses were set to unity so that forces were easily calculated from displacements. No measurable error resulted between the force and moment outputs from the mechanism in ABAQUS and the fastener element in the frame code, demonstrating the geometry and coupling assumed are appropriate. A second verification of the model was completed using MASTAN2 (McGuire et al. 2000). The purpose was to verify if the fastener element provided the same basic coupling as an Euler-Bernoulli beam element. A single beam element was exercised with the same unit displacements as Fig. 1 and the results for element local forces in showed that the axial stiffness k_z was equivalent to EA/L, the shear stiffness k_y was equal to $12EI/L^3$, the rotational stiffness $k_{\varphi x}$ was equal to $4EI/L$, and all of the coupled and remaining terms agreed with Euler-Bernoulli Theory as well. A fastener element validation was not performed, but can be possible

when an extensive suite of fastener tests are performed, and a large collection of multi-directional stiffnesses are available.

2.3 Frame Analysis Implementation and Study Problem

The derived fastener element is implemented in an in-house two-dimensional beam finite element code programmed in Matlab (2014). The beam element is a standard 2D Euler-Bernoulli beam element with 6 degrees of freedom and includes both the elastic and geometric stiffness matrix (see, e.g., McGuire et al. 2000). This code is used to create a model of a built-up cold-formed steel column where the individual members are modeled using the 2D beam finite elements and the fasteners connecting the individual members are modeled with the derived fastener element.

A back-to-back cold-formed steel lipped channel is selected as the study problem. The selected column length is 10 ft [3.1 m], the flexural properties of a standard 600S162-54 stud section (see AISI-S200 [2012] for nomenclature) are used for the individual members. A fine mesh of 240 beam elements (0.5 in [1.27 cm] in length) per stud was used for convenience. Also, a globally-pinned boundary condition was applied to the columns. This was implemented by restricting longitudinal motion at the member mid-length, and restricting only transverse displacement at the end nodes of the columns, as illustrated in the first mode buckled shape of Fig. 4.

Shear slip at fastener locations is regarded as an important component of built-up member deformation. Localized, relative member displacement is shown in Fig. 4 where columns are represented by their centroidal axes. The shear spring k_y is assumed to be the fastener stiffness with the greatest contribution to the degree of compositeness for the built-up section. A small parametric study was performed in which k_y, k_z, and $k_{\varphi x}$ fastener stiffnesses were varied and combined in multiple trials; only the shear spring offered a meaningful variation in the buckling load for the deformation modes considered. In this work only sympathetic flexural global buckling shapes of the connected members are considered, so the rotational spring $k_{\varphi x}$ is not activated in these analyses. Therefore its stiffness is set to zero in this preliminary work. The axial spring, k_z, enforces the desired sympathetic buckling modes (i.e. where the two individual members buckle in the same pattern and in the same direction) if it is set to a high enough value. In this study the fasteners are assumed axially rigid and a stiffness of 1000 kip/in [175 kN/mm] is employed. Fig. 5 shows the implementation of the fastener element.

Recent stud-fastener-stud shear tests (Moen et al. 2014) provide an estimate of the shear stiffness, k_y. The observed deformation includes tilting and bearing, and at higher loads or deformations screw shear and screw pull-out. The results are dependent on the thickness of the studs, fastener diameter, and additional fastener details (thread pitch, shank length, etc.). In total the results indicate shear stiffness, k_y, for individual fasteners between 20-30 kip/in [3.5-5.3 kN/mm]. The shear stiffness is systematically varied in the majority of parameter studies herein; when set to a constant, a value of 30 kip/in [5.3 kN/mm] is used.

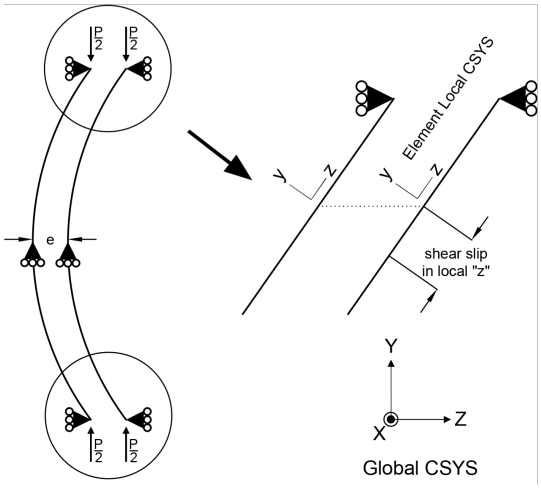

Figure 4: Shear slip seen in flexural buckling

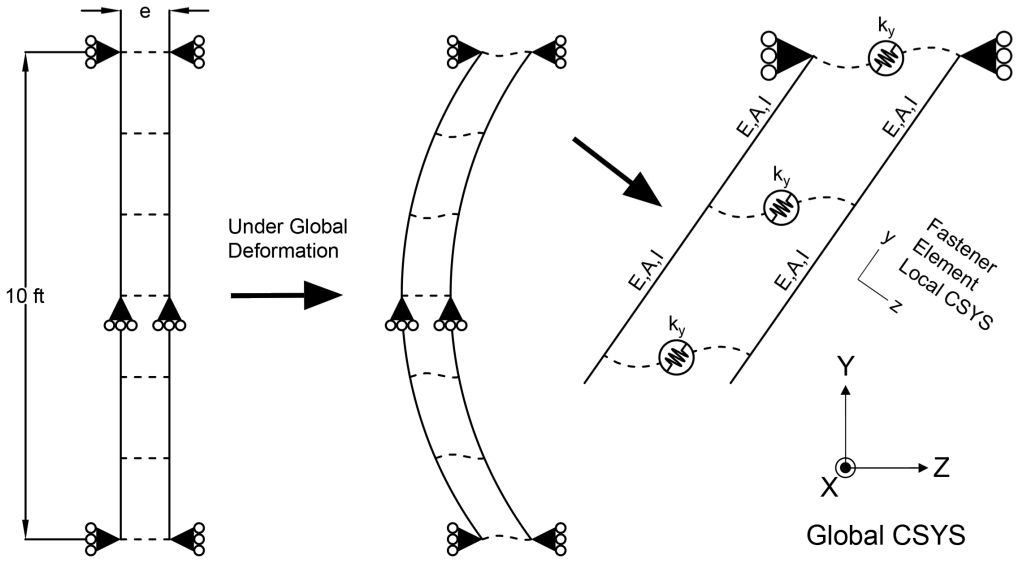

Figure 5: Implementation of the fastener element

2.4 Developing a Compositeness Parameter: β

Since the estimation of partially composite action is currently not available in design codes, other than the calculation of modified slenderness as discussed previously, the authors sought a numerical approach to calculating the level of compositeness; a parameter calculated herein as β. Member end conditions, mode of global deformation, fastener spacing, the presence of fastener end groupings, and fastener stiffness all influence β. Consider a model of a composite column such as depicted in Fig. 5. An eigen-buckling stability analysis is performed and the buckling load (P_{cr}) and mode shape (n) recorded.

Theoretically, the buckling load is:

$$P_{cr} = \frac{(n\pi)^2 EI_{PC}}{L^2} \tag{2}$$

where L is the member length, E is the (steel) member modulus of elasticity, and I_{PC} is the partially composite moment of inertia for the built-up section. For a given model (i.e., given fastener stiffness, layout, etc.) P_{cr} and n are known, so I_{PC} may be back-calculated.

The partially composite moment of inertia may be written as:

$$I_{PC} = 2I_o + \beta(\tfrac{1}{2}Ae^2) \tag{3}$$

where I_o is the moment of inertia of a single stud in the section about its own minor axis, A is the area of a single stud, and e is the distance between both studs' centroids. The parameter β may be back-calculated and provides a measure of the degree of compositeness with 0 being non-composite and 1 being fully composite.

2.3 AISI fastener layout requirements

The objective of this work is to understand the impact of fastener stiffness and layout (spacing). For our studied problem, one important fastener layout is that prescribed by AISI-S100-12. AISI-S100-12 Section D1.2 specifies a prescriptive group of fasteners at the ends (see Fig. 6 - at the ends, fasteners must be longitudinally spaced no more than 4 diameters apart and for a distance equal to 1.5 times the maximum width of the member) and a maximum fastener spacing, a, along the length via:

$$\frac{a}{r_i} \le \frac{1}{2}\left(\frac{KL}{r}\right)_o \tag{4}$$

For the studied 600S162-54 section at L of 10 ft [3.05 m], r_i is 0.569 in. [14.5 mm] and $(KL/r)_o$ is 174.6 in. [4.43 m] for K=1. This results in an a of 50.0 in. [1.3 m], or about $L/3$ for the studied built-up column. For the end fasteners, if the diameter of the screws (assuming #8 self-drilling, steel-to-steel tapping screws are used whose diameter is about 0.164 in. [4.2 mm], but conservatively reduced to $^1/_8$ in. [3.2 mm]), if fasteners at the edges of the members are omitted due to constructability constraints, and if the maximum width of the member is taken as the web depth of 6 in. [152 mm], the required number of fasteners becomes 9 rows of fastener pairs spaced at 0.5 in. [13 mm], as illustrated in Fig. 6 and used in the parametric studies presented herein.

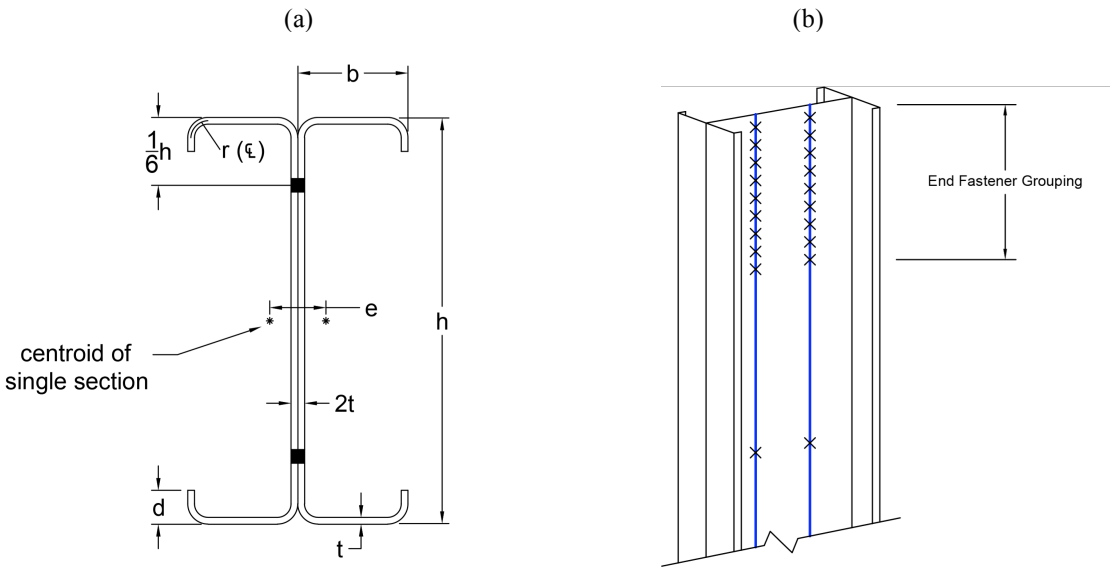

Figure 6: (a) The built-up, back-to-back section with 600S162-54 studs, where e = 0.848 in [21.5 mm] and (b) an example of the AISI-recommended fastener layout

3. Numerical Analysis Results

3.1 Fastener Sensitivity Buckling Study

Eigen-buckling analysis was completed with the developed finite element model for the back-to-back 600S162-54 built-up column with a fastener placed at each node for this study only (see Fig. 7). To explore the sensitivity of the model to fastener location, analyses were completed where individual fasteners were removed and the change in the buckling load recorded. Specifically, a sensitivity parameter, Ω, was calculated as shown in Eq. 5.

$$\Omega = \frac{P_{cr,n} - P_{cr,n-i}}{P_{cr,n}} \tag{5}$$

where $P_{cr,n}$ refers to the buckling load of the built-up column with all "n" fasteners present, and $P_{cr,(n-i)}$ represents the buckling load when fastener "i" is removed. Sensitivities to fastener location in the first and second mode are provided in Fig. 7. In general individual fastener removal has only a modest impact on the buckling load; however, the locations where shear deformations are largest (ends in mode 1, middle in mode 2) are relatively the most important. In addition, the relative importance of a given location is greatest when the shear stiffness of the fasteners is lower – if the fastener stiffness is high the loss of an individual fastener has little impact.

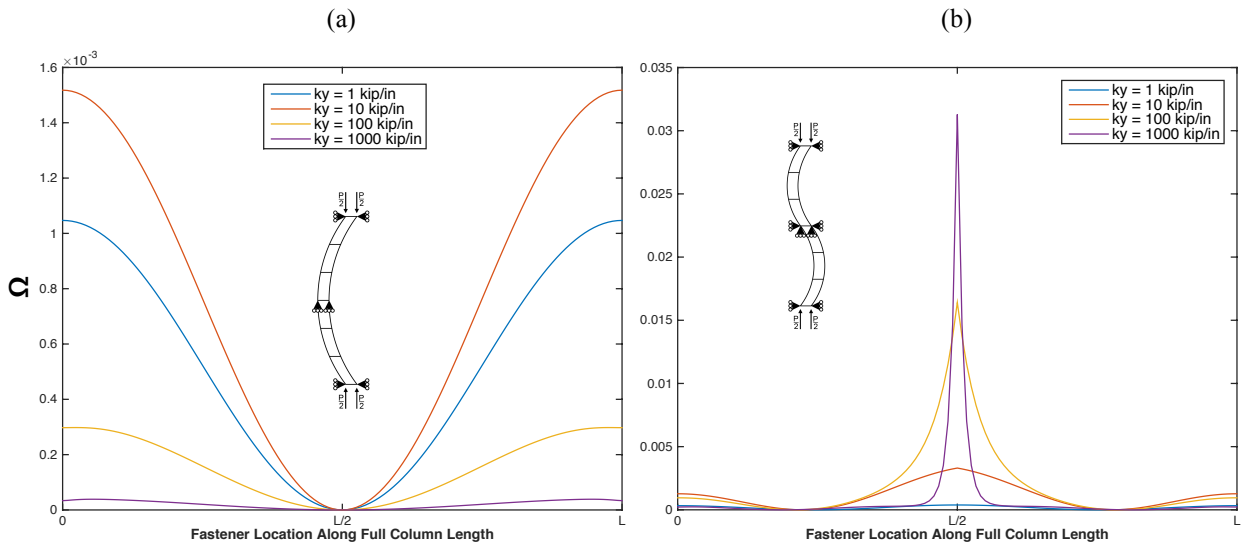

Figure 7: Omega, fastener sensitivity results for (a) buckling mode 1 and (b) buckling mode 2

3.2 Fastener Stiffness and Layout Buckling Study

Eigen-buckling analysis was completed for the back-to-back 600S162-54 built-up column for a range of 29 different fastener shear stiffnesses k_y (ranging from 0-1000 kips/in [0-175 kN/mm]) and a suite of 17 even fastener spacings, ranging from $L/1$ (only one fastener on either end of the column) to $L/240$ (one fastener every 0.5 in. [12.7mm]). A complementary parametric study was completed with a fastener layout that follows recommendations in AISI-S100-12, specifically the large fastener grouping at the member ends. Typical buckling mode shapes for both studies are provided in Fig. 8. Classical global flexural buckling mode shapes are observed for the first and higher modes. In the results that follow, only the first mode results are provided for brevity.

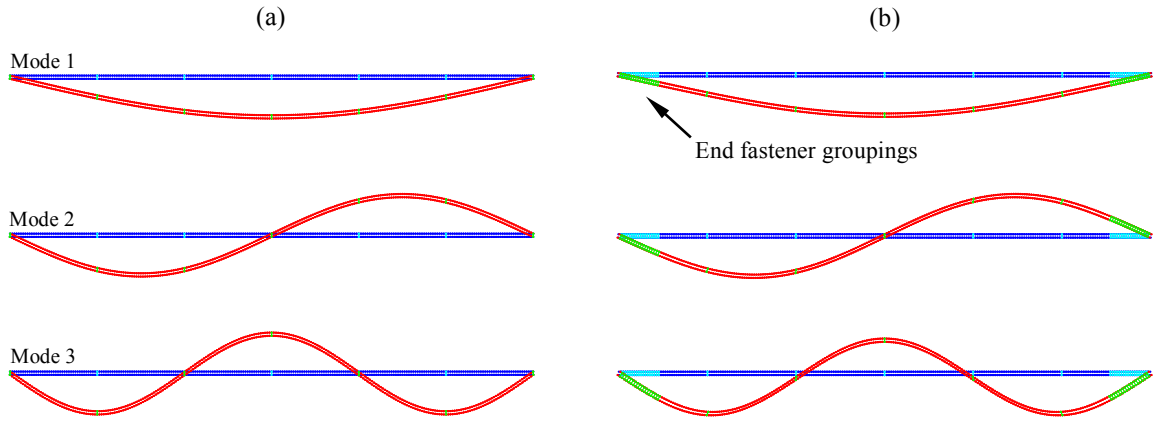

Figure 8: Buckling mode outputs with (a) a sample $L/6$ even fastener spacing and (b) with added end groupings

Detailed examination of the buckled shapes, particularly at the member ends is important for fully understanding the impact of the fastener shear stiffness on the response. Fig. 9 provides detailed deformed shapes at the member ends without (Fig. 9a-b) and with (Fig. 9c-d) the special AISI end fastener grouping. For low levels of fastener shear stiffness, shear deformation between the two individual members is observed, but as the fastener stiffness increases the shear deformation decreases until essentially the classic composite condition of plane sections remaining plane even between the two members is achieved.

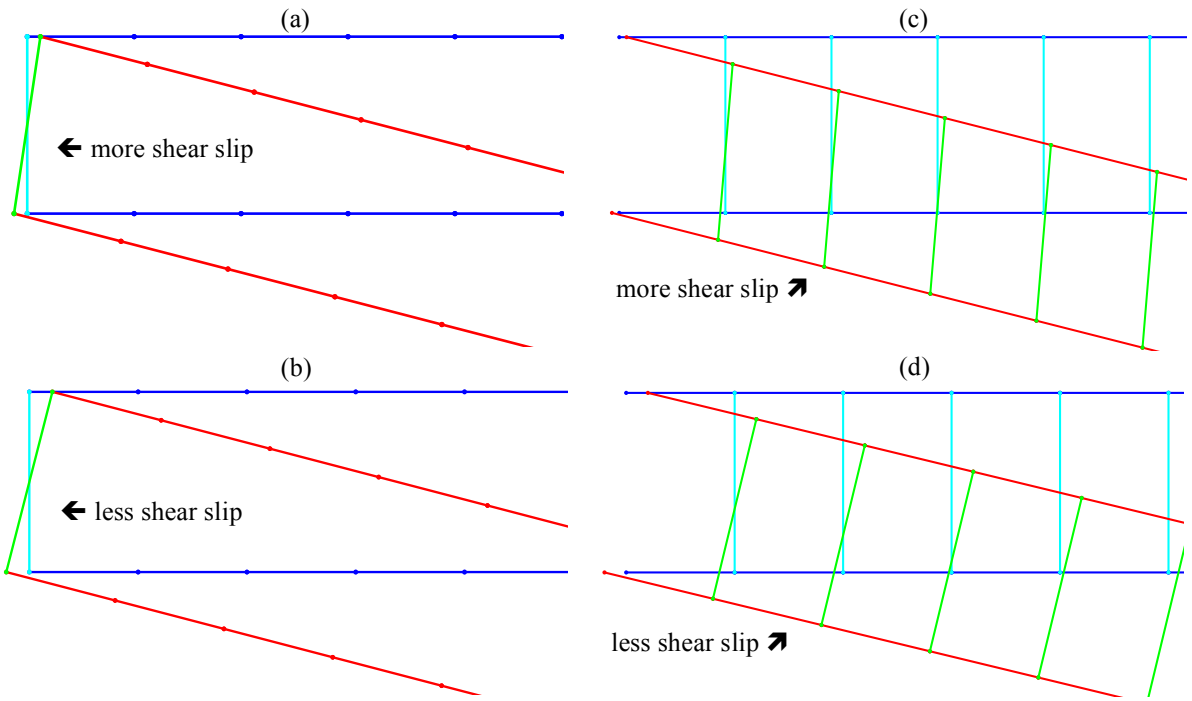

Figure 9. Examples of undeformed (blue) and deformed (red) geometry:
with (a) low k_y and (b) high k_y with even fastener spacing, and (c) low k_y and (d) high k_y with the AISI layout

The first mode elastic buckling loads for all studied sections are summarized Fig. 10. The individual fastener stiffness is systematically increased for a variety of different fastener spacing both without (Fig. 10a) and with (Fig. 10b) the end fastener detailing prescribed in AISI-S100-12. Also in Fig. 10, for the built-up back-to-back 600S162-54, the non-composite lower limit (7.28 kips [32.4 kN]) and fully composite limit (11.13 kips [49.5 kN]) are provided. AISI-S100-12 Section D1.2 requires approximately *L*/3 spacing along the length so trials with *L*/3 fastener spacing are provided with a thicker line in Fig. 10 and the modified slenderness (Eq. 1) AISI buckling prediction is also provided.

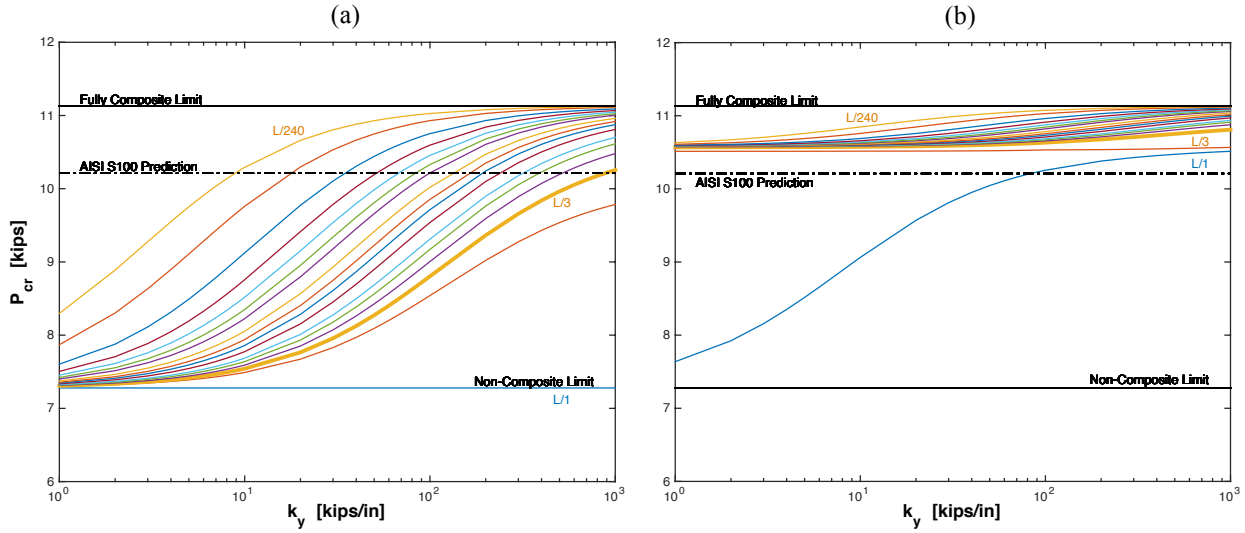

Figure 10: Buckling load results with (a) even fastener spacing and (b) AISI-based fastener layout

Fig. 10a illustrates the model is capable of capturing the full range of behavior from non-composite to fully composite. Fig. 10b illustrates the profound impact of the end fastener detail of AISI-S100-12. As long as an intermediate fastener is provided the end detailing itself is adequate for reaching the AISI-S100-12 predicted P_{cr}, essentially independent of fastener stiffness. The Fig. 10 results may be illustrated in terms of the compositeness parameter, β, as provided in Fig. 11. Again, each curve corresponds to different fastener spacings. For even fastener spacing without special end details (Fig. 11a), and for the most realistic level of fastener stiffness (between 10-100 kips/in [1.75-17.5 kN/mm]) there exists a large potential range of β, covering at least 75% of the potential amount of composite action, depending on fastener spacing. The expected trend of approaching the fully composite condition with tighter fastener spacing and higher fastener stiffness is also clear. When the AISI-S100-12 end conditions are included, and as long as an intermediate fastener is provided, then a minimum of 85% composite action is achieved as shown in Fig. 11b.

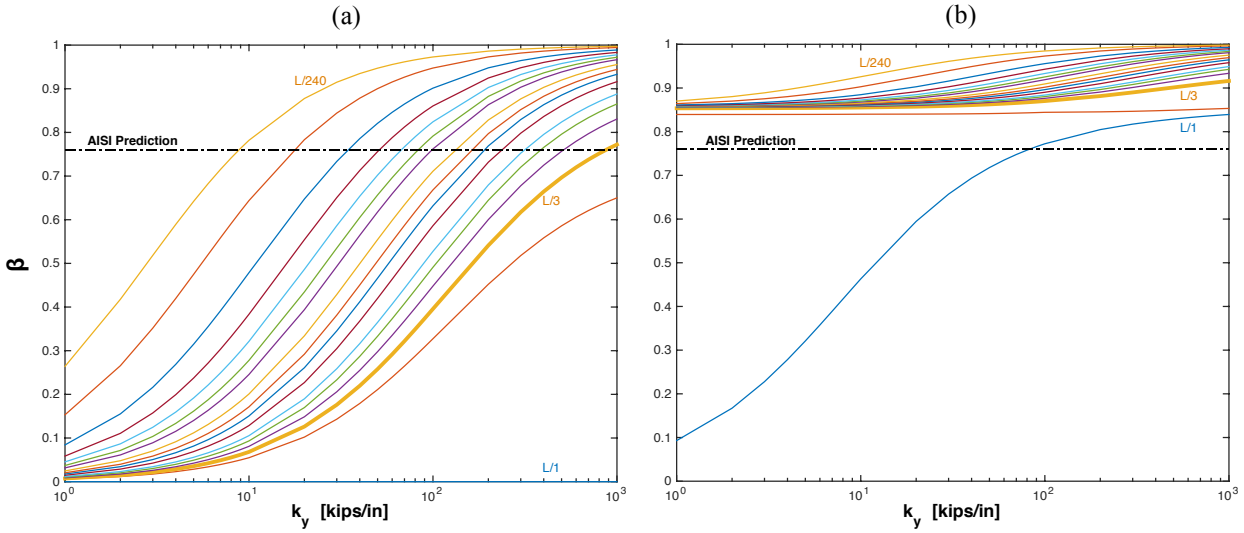

Figure 11: β results with (a) even fastener spacing and (b) AISI-based fastener layout

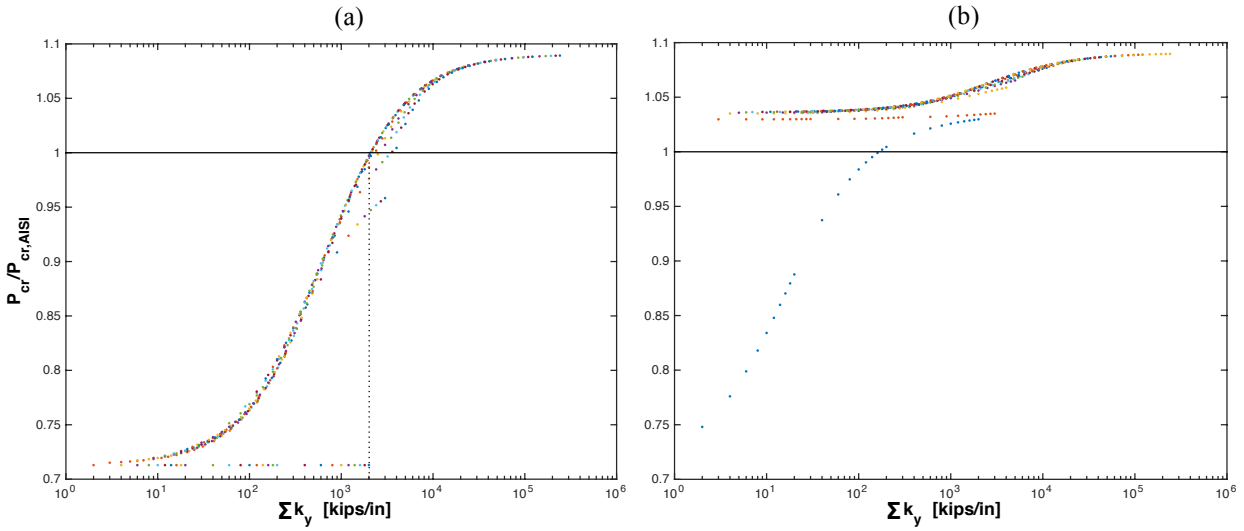

Figure 12: Normalized buckling results vs. summed fastener stiffness per member, with (a) even fastener spacing and (b) AISI-based fastener layout, note Σk_y does not include end grouping

The results of the parametric study can be simplified if one considers the total shear stiffness provided instead of the individual fastener stiffness. Fig. 12 provides the flexural buckling load as normalized to the AISI prediction and as a function of the summation of the fastener stiffness per model. With the exception of the $L/1$ spacing (fasteners at ends only) and the $L/2$ spacing (fasteners at ends and middle only) the results cluster along a function indicating that for any reasonable fastener spacing the total stiffness provided is the most important parameter. Also, from Fig. 12a it may be understood that a cumulative shear stiffness of about 2000 kips/in [350 kN/mm] provides the shear stiffness equivalent to the AISI modified slenderness ratio.

3.3 Static Analysis Results

For the design of composite members in bending, the classic methodology is to assume the section is fully composite (FC) and then determine the stress on the plane where connectors are located that combine the two sections. Elementary beam theory (which presumes ideal fully composite shear response) is utilized. This method provides a means to predict the relative shear demand on the fasteners which connect the member and is explored here in relation to the model results developed where shear deformation and other fastener details are allowed.

Classic design for composite members uses elementary beam theory of the form:

$$q(y) = \frac{\tau(y)}{b} = \frac{V(y)Q_{FC}}{I_{FC}} \tag{6}$$

where $q(y)$ is the shear flow along the length at the plane where the fasteners connect the members (i.e. the cut plane), $\tau(y)$ is the shear stress at the cut plane, b is the width at the cut plane, $V(y)$ is the transverse shear demand, Q_{FC} is the fully composite first moment of area from the cut plane, and I_{FC} is the fully composite moment of inertia.

For the stability results herein the deformations, w, are near to the ideal elastic buckling modes:

$$w(y) \cong B\sin\left(\frac{m\pi y}{L}\right) \tag{7}$$

where B is the amplitude of the mode and m is the mode number. From this transverse deformation the transverse shear, $V(y)$ can be estimated:

$$V(y) \cong -BEI_{FC}\left(\frac{m\pi}{L}\right)^3 cos\left(\frac{m\pi y}{L}\right) \text{ or } BEI_{FC}\left(\frac{m\pi}{L}\right)^3 \left|cos\left(\frac{m\pi y}{L}\right)\right| \tag{8}$$

Using $V(y)$ an engineering approximation to the shear flow can be made by substituting Eq. 8 into Eq. 6. where B is the amplitude of the mode and m is the mode number. The shear flow at a fastener location may be multiplied times its tributary length to estimate demands on a given fastener.

$$q(y) \cong \frac{BEI_{FC}\left(\frac{m\pi}{L}\right)^3\left|cos\left(\frac{m\pi y}{L}\right)\right|Q_{FC}}{I_{FC}} \quad \text{(analytical approximation)} \tag{9}$$

Alternatively from the model itself one can determine the shear flow. This is completed most readily by finding the shear force in fastener '*i*' ($F_{shear}(y_i)$) and dividing by the tributary length for that fastener, i.e.:

$$q(y_i) = \frac{F_{shear}(y_i)}{\ell_{trib}} \quad \text{(model)} \tag{10}$$

The amplitude of a buckling mode is arbitrary, but if it is held to a constant value (e.g. B = 1 in. [25.4 mm]), then the approximation from Eq. 9 can be readily compared to the model results of Eq. 10. These two shear flow approximations are compared for the parametric study without (Fig. 13a-b) and with (Fig. 13c-d) the AISI end fastener details at a k_y = 30 kip/in [5.3 kN/mm].

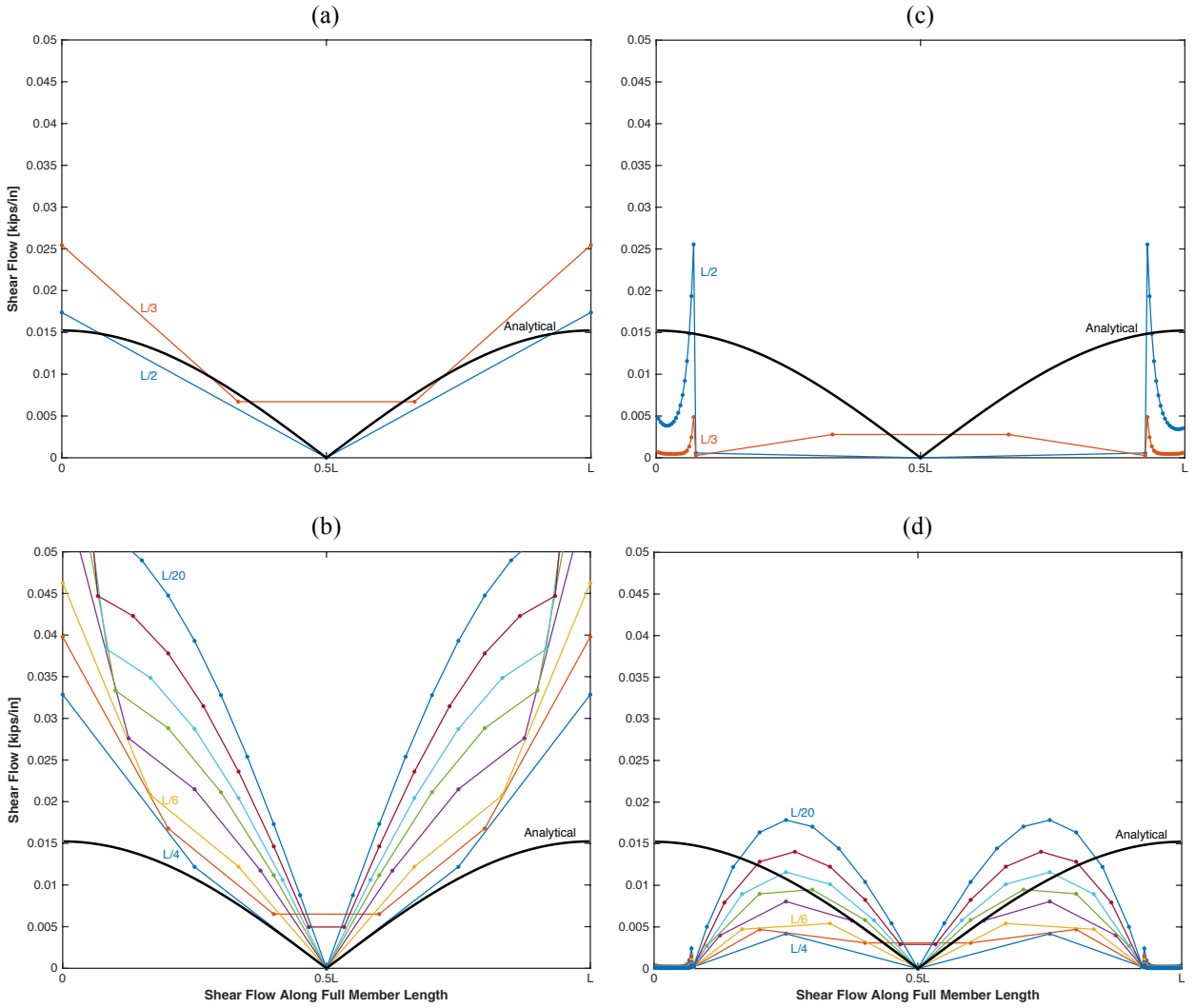

Figure 13: Analytical and numerical fastener shear flow results for even fastener spacing trials: with (a) *L*/2-*L*/3 and (b) *L*/4-*L*/20 spacings, and AISI fastener layouts with (c) *L*/2-*L*/3 and (d) *L*/4-*L*/20 spacings

The force levels in Fig. 13 are necessarily arbitrary (since the magnitude of the buckling mode itself is arbitrary) so the worth of Fig. 13 is in the shape of the shear flow and comparison between the analytical approximation and the model, not the absolute magnitudes. For the models without special end conditions (Fig. 13a-b) the fastener forces near the ends are significantly higher than the simplified engineering theory predicts indicating the importance of understanding slip at the member ends for the forces developed, in addition to the stiffness provided. When the special end conditions are supplied, force levels are reduced and the analytical approximation gives a reasonable estimation of the observed shear flow. It is worth noting that in higher modes it is not only the ends that are locations of high importance for shear.

4. Discussion

The effect of the AISI end fastener grouping is profound. All of the analysis results indicate this; however, it is also an expensive detail and one not favored by industry or practice. To what extent this detail could be optimized while still maintaining adequate performance is a worthwhile topic that the provided model could potentially evaluate. The preliminary examination of fastener forces (shear flow) indicates that simplified models may be challenged to provide accurate estimate of fastener demands for design. To explore this fully, at a minimum, second-order elastic analyses of the model undergoing large deformations is needed, and is possible.

Although the provided model covers flexural buckling, cold-formed steel members also suffer from torsional-flexural buckling and this needs to be considered as the impact of torsion on the stiffness demands for the connecting elements in the built-up section is poorly understood. Preliminary work investigating the impact of fastener layout on local and distortional buckling has been completed in other work of the senior author, but significant work remains. In particular, developing efficient finite strip solutions that include shear slip at connections between members is highly desired.

An unstated hypothesis of this work is that a useful correlation exists between elastic buckling and strength. While this has been long proven for isolated members, for partially composite sections with significant shear deformation it is unknown if the usual column curves, etc., will remain appropriate. To this end, both experiments and nonlinear finite element collapse analysis models are needed to fully explore the strength of built-up members.

This work and previous work of the authors provides the first tentative steps towards improving built-up member design for cold-formed steel members, but a comprehensive design approach that allows the engineer to fully optimize the selected fasteners and their location for all relevant buckling modes is still sought and remains a goal for the effort.

5. Conclusions

Using a simple element to capture fastener stiffness, it is possible to discretely model flexural buckling of built-up members with full consideration of shear deformations in the connecting elements, as well as the impact of fastener stiffness and spacing/layout along the length of the member. Fully composite built-up members can be difficult and expensive to achieve. In many cases practical details lead to partially composite members and thus, engineers need a means to assess and utilize these members. A small two-dimensional beam finite element model with a

special fastener element utilized to connect two beam elements together is employed in static and eigen-buckling analysis to explore the behavior of cold-formed steel built-up sections in global flexural buckling. The model is able to capture the full range of behavior from non-composite to fully-composite depending on fastener stiffness and layout. In addition, the specific details of the fastener layout from the AISI-S100-12 Specification are studied. The prescriptive end fastener layouts from AISI-S100-12 are shown to have a profoundly positive impact on the buckling performance of the member. Ultimately, the goal of the research is to provide an analysis-based design method for cold-formed steel built-up sections that can be used to design and optimize unique and efficient cold-formed steel built-up sections Much work remains towards this goal.

Acknowledgements

Research for this paper was conducted with Government support under FA9550-11-C-0028 and awarded by the Department of Defense, Air Force Office of Scientific Research, National Defense Science and Engineering Graduate (NDSEG) Fellowship, 32 CFR 168a.

References

ABAQUS 6.13-2, 2013, Dassault Systèmes Simulia Corp., Providence, RI.

AISC 360 (2010). *Specification for Structural Steel Buildings*, American Institute of Steel Construction, Chicago, IL.

AISI-S100. (2012). *North American Specification for the Design of Cold-Formed Steel Structural Members*, American Iron and Steel Institute, Washington, D.C.

AISI-S200. (2012). *North American Standard for Cold-Formed Steel Framing – General Provisions*, American Iron and Steel Institute, Washington, D.C.

Aslani, F. and Goel, S.C. (1991). "An Analytical Criterion for Buckling Strength of Built-up Compression Members." *Engineering Journal*, 28(4),159-168.

Duan, L., Reno, M., Uang, C-M. (2002). "Effect of Compound Buckling on Compression Strength of Built-up Members." *Engineering Journal*, 39(1), 30-37.

Fratamico, D.C. and Schafer, B.W. (2014). "Numerical Studies on the Composite Action and Buckling Behavior of Built-Up Cold-Formed Steel Columns." *22nd International Specialty Conference on Cold-Formed Steel Structures*, St. Louis, MO.

Georgieva, I., Schueremans, L., Vandewalle, L., Pyl, L. (2012). "Design of built-up cold-formed steel columns according to the direct strength method." *Procedia Engineering*, 40, 119-124.

Kalochairetis, K. and Gantes, C. (2011). "Numerical and analytical investigation of collapse loads of laced built-up columns." *Computers & Structures*, 89, 1166-1176.

Li, Yuanqi, Li, Yinglei, Wang, S., Shen, Z. (2014). "Ultimate load-carrying capacity of cold-formed thin-walled columns with built-up box and I section under axial compression." *Thin-Walled Structures*, 79, 202-217.

Li, Z. and Schafer, B.W. (2010a). "Buckling analysis of cold-formed steel members with general boundary conditions using CUFSM: conventional and constrained finite strip methods." *20th International Specialty Conference on Cold-Formed Steel Structures*, St. Louis, MO.

Liu, J.L., Lue, D.M., Lin, C.H. (2009). "Investigation on slenderness ratios of built-up compression members." *Journal of Constructional Steel Research*, 65(1), 237-248.

Loughlan, J. and Yidris, N. (2014). "The local-overall flexural interaction of fixed-ended plain channel columns and the influence on behaviour of local conditions at the constituent plate ends." *Thin-Walled Structures*, 81, 132-137.

Maia, W.F., et al. (2012). "Numerical and Experimental Investigation of Cold-Formed Steel Double Angle Members Under Compression." *21st International Specialty Conference on Cold-Formed Steel Structures*, St. Louis, MO.

MATLAB 2014b, The MathWorks, Inc., Natick, MA, United States.

McGuire, W., Gallagher, R., Ziemian, R. *Matrix Structural Analysis*. New York, NY: John Wiley & Sons, Inc., 2000. Print.

Moen, C.D., et al. (2014). "Towards Load-Deformation Models for Screw-Fastened Cold-Formed Steel-to-Steel Connections." *22nd International Specialty Conference on Cold-Formed Steel Structures*, St. Louis, MO.

Peköz, T. (1990). "Design of Cold-Formed Steel Screw Connections." *10th International Specialty Conference on Cold-Formed Steel Structures*, St. Louis, MO.

Piyawat, K., Ramseyer, C., Kang, T.H-K. (2011). "Nonlinear buckling of built-up cold-formed steel sections." *International Journal of Theoretical and Applied Multiscale Mechanics*, 2(2), 146-164.

Post, B. (2012). "Fastener Spacing Study of Cold-Formed Steel Wall Studs Using Finite Strip and Finite Element Methods." Master's Essay, The Johns Hopkins University, Baltimore, MD.

Schafer, B.W. and Ádàny, S. (2006). "Buckling analysis of cold-formed steel members using CUFSM: conventional and constrained finite strip methods." *18th International Specialty Conference on Cold-Formed Steel Structures*, Orlando, FL.

Stone, T.A. and LaBoube, R.A. (2005). "Behavior of cold-formed steel built-up I-sections." *Thin-Walled Structures*, 43(12), 1805-1817.

Young, B. and Chen, J. (2008). "Design of Cold-Formed Steel Built-Up Closed Sections with Intermediate Stiffeners." *Journal of Structural Engineering*, 134, 727-737.

Zhang, J. *Cold-formed steel built-up compression members with longitudinal stiffeners*. Dissertation, The University of Hong Kong; 2014.